Polyketides from the marine-derived fungus *Ascochyta salicorniae* and their potential to inhibit protein phosphatases

Simon F. Seibert,[a] Ekaterina Eguereva,[a] Anja Krick,[a] Stefan Kehraus,[a] Elena Voloshina,[b] Gerhard Raabe,[b] Jörg Fleischhauer,[b] Eckhard Leistner,[a] Michael Wiese,[c] Heino Prinz,[d] Kirill Alexandrov,[d] Petra Janning,[d] Herbert Waldmann[d] and Gabriele M. König*[a]

Received 30th January 2006, Accepted 20th March 2006
First published as an Advance Article on the web 3rd May 2006
DOI: 10.1039/b601386d

Chemical investigation of the marine fungus *Ascochyta salicorniae* led to the isolation of two new epimeric compounds, ascolactones A (**1**) and B (**2**), in addition to the structurally-related polyketides hyalopyrone (**3**), ascochitine (**4**), ascochital (**5**) and ascosalipyrone (**6**). The absolute configurations of the epimeric compounds **1** and **2** were assigned as (1*R*,9*R*) and (1*S*,9*R*), respectively, through simulation of the chiroptical properties using quantum-chemical CD calculations, and chiral GC–MS subsequent to oxidative cleavage (Baeyer–Villiger oxidation) of the side chain.
In silico screening using the PASS software identified some of the *A. salicorniae* compounds (**1**–**6**) as potential inhibitors of protein phosphatases. Compound **4** was found to inhibit the enzymatic activity of MPtpB with an IC_{50} value of 11.5 μM.

Introduction

Protein phosphatases have emerged as promising drug targets for a wide range of diseases. Eucaryotic phosphatases are involved in signal transduction pathways with influence on pathogenic mechanisms, *e.g.* Cdc25 (cell division cycle 25) phosphatase plays a role in neoplastic events, and PTP1B (protein tyrosine phosphatase 1B) is involved in type 2 diabetes.[1,2] Some procaryotic phosphatases are assumed to influence the pathogenicity of bacteria such as *Yersinia pestis* and *Mycobacterium tuberculosis*. Inhibition of the phosphatase MPtpB (*M. tuberculosis* protein tyrosine phosphatase B) impairs mycobacterial survival in IFN-γ activated macrophages and in guinea pigs, which makes this enzyme a putative new target for antimycobacterial drugs.[3,4]

Marine natural products are regarded as promising sources of new phosphatase inhibitors. The sponge metabolites sulfircin and coscinosulfate inhibit the eucaryotic dual specificity phosphatase Cdc25A,[5,6] and pulchellalactam[7] from the marine fungus *Corollospora pulchella* inhibits CD45 (cluster of differentiation 45), a receptor-like transmembrane phosphatase, associated with autoimmune and chronic inflammatory diseases. To date, however, no marine natural products have been evaluated for activity towards procaryotic protein phosphatases, such as MPtpB.

A culture of the fungus *Ascochyta salicorniae* was isolated from the marine alga *Ulva* sp. collected from the North Sea near Tönning, Germany. Surface sterilization of the algal thalli before incubation of the algal material on suitable agar medium ensured that the fungus obtained was present inside the algal tissue, *i.e.* was endophytic. Cultivation of this fungus under various conditions showed it to have a very diverse secondary metabolism, being able to produce several polyketides and alkaloids with pronounced antimicrobial activity.[8] During the current study, *in silico* screening studies using the PASS (prediction of activity spectra for substances) software[9] showed some of the polyketides identified to be potential inhibitors of protein phosphatases. In order to verify this *in silico* result, polyketides from *A. salicorniae* were isolated and tested towards a broad range of phosphatases.

Results and discussion

The fungus was cultivated on solid, seawater-containing medium and yielded, after extraction and successive fractionation by vacuum liquid chromatography (VLC) and normal and reversed phase HPLC, the polyketide metabolites **1**–**6** (Chart 1). Compounds **1** and **2** are two new epimeric lactones, named ascolactone A (**1**) and ascolactone B (**2**). Compounds **3**–**6** were identified as the known metabolites hyalopyrone, ascochitine, ascochital and ascosalipyrone, respectively.[8,10–14] ^{13}C NMR data evidenced compound **5** as well as compound **6** to be mixtures of chromatographically inseparable diastereomers as described formerly for samples obtained from *Kirschsteiniothelia maritima* and *A. salicorniae*, respectively.[8,14]

Ascolactone A (**1**) was found to have the molecular formula $C_{15}H_{16}O_7$ as deduced by ESI-MS and high resolution EI-MS. The UV maximum at 311 nm was characteristic of an extended aromatic ring, whereas IR and the ^1H NMR data (ν_{max} 3443, 1716, 1718 cm^{-1}; δ 17.28 for OH-4; δ 14.73 for OH-6) indicated the presence of carbonyl and hydroxy groups within the molecule. Seven of the eight elements of unsaturation deduced from the molecular formula can be attributed to the aromatic moiety of the molecule [C-6 (δ 170.8), C-4 (δ 166.9), C-7a (δ 154.9), C-5 (δ 104.3), C-3a (δ 102.0), C-7 (δ 99.1)), and to three carbonyl groups,

[a]*Institute for Pharmaceutical Biology, University of Bonn, Nußallee 6, D-53115 Bonn, Germany. E-mail: g.koenig@uni-bonn.de; Fax: +49 228 733250; Tel: +49 228 733747*
[b]*Institute for Organic Chemistry, Rheinisch-Westfälische Technische Hochschule Aachen, Landoltweg 1, D-52074 Aachen, Germany*
[c]*Pharmaceutical Institute, University of Bonn, An der Immenburg 4, D-53121 Bonn, Germany*
[d]*Max Planck Institute of Molecular Physiology, Otto-Hahn-Straße 11, D-44227 Dortmund, Germany*

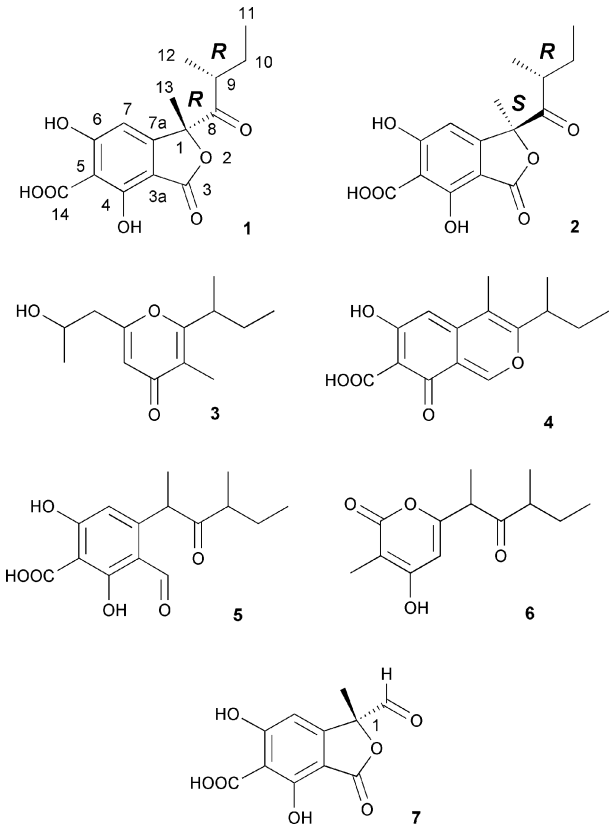

Chart 1 Secondary metabolites isolated from *A. salicorniae* and model compound (**7**) for quantum-chemical calculations.

i.e. C-8 (δ 210.6), C-14 (δ 176.7) and the lactone carbonyl C-3 (δ 170.1). Compound **1** thus had to be bicyclic.

The aromatic region of the ^{1}H NMR spectrum of **1** revealed a singlet (H-7, δ 6.12) of a penta-substituted benzene. Only one ^{1}H–^{1}H spin-system, H_3-11 through to H_3-12, could be deduced from a ^{1}H–^{1}H COSY experiment, and showed the presence of a 2-substituted butyl residue within the molecule. A singlet resonance at δ 1.65 in the ^{1}H NMR spectrum of **1** indicated the presence of a tertiary methyl group (C-13) bound to an oxygenated carbon atom. HMBC correlations from both H_3-12 and H_3-13 to the carbonyl carbon C-8, and from H_3-13 to C-7a connected the side chain to the aromatic ring. HMBC correlations from H-7 to C-8 and C-1 positioned this side chain *ortho* to H-7. This regiochemistry was confirmed by an NOE observed between H-7 and H_3-13. Further HMBC correlations were detected between carbonyl carbon C-3 and the hydroxy proton OH-4, indicating the lactone carbonyl to be bound to C-3a of the aromatic ring. This was in good agreement with the low-field shift of the ^{1}H NMR signal for OH-4, due to a hydrogen bridge between the lactone carbonyl and OH-4. This left the substitution of positions 5 and 6 of the aromatic ring with either a hydroxy or carboxyl function to be deduced. The substitution pattern of the aromatic ring was not easily established due to the scarcity of hydrogens within this part of the molecule, resulting in limited information obtained from the HMBC correlations. Strong HMBC correlations of OH-6 with C-7 and C-5 pointed, however, towards a substitution pattern with *meta*-positioned OH groups and the carboxylic function at C-5. HPLC separation yielded a second compound (**2**) with a planar structure identical to that of ascolactone A (**1**). In this case the vicinal relationship between H-7 and OH-6 could be shown by an NOE between these two protons, confirming the above conclusions regarding the regiochemistry of the compounds.

Significant differences in the ^{1}H and ^{13}C NMR spectra (Table 1) as well as the chromatographic separation of the two compounds on achiral phases indicated that ascolactone A (**1**) and B (**2**) had to be epimeric, either at C-1 or C-9.

The CD spectra (Fig. 1) of **1** and **2** are virtually mirror images. Time-dependent density functional theory (TDDFT) offers a strategy to elucidate the absolute configuration of molecules by comparing measured and calculated CD spectra.[15] Thus, in order to assign the absolute configuration at the chiral centers C-1 and

Table 1 ^{1}H and ^{13}C NMR data for compounds **1** and **2** (δ in ppm, J in Hz)

	1 [a]				**2** [a]			
No.	δ ^{13}C [b]	δ ^{1}H [c] (mult., J)	HMBC [d]	NOE [e]	δ ^{13}C [b]	δ ^{1}H [c] (mult., J)	HMBC [d]	NOE [e]
1	90.2 C				89.6 C			
3	170.1 C				170.0 C			
3a	102.0 C				101.9 C			
4	166.9 C				167.0 C			
5	104.3 C				104.4 C			
6	170.8 C				170.9 C			
7	99.1 CH	6.12 (s)	1, 3, 3a, 4, 5, 6, 8, 14	9, 11, 13	99.0 CH	6.12 (s)	1, 3, 3a, 4, 5, 6, 8, 14	6-OH, 13
7a	154.9 C				155.6 C			
8	210.6 C				210.9 C			
9	42.4 CH	2.71 (m)	8, 10, 11[f], 12	7, 10a, 11, 12, 13	42.2 CH	2.80 (m)	8, 10, 12	7, 10a, 10b, 11, 12
10	26.5 CH_2	1.43 (Ha, m)	9, 11, 12	7, 9, 11, 12	26.9 CH_2	1.68 (Ha, m)	8, 9, 11, 12	9
		1.16 (Hb, m)	9, 11, 12	9, 11, 12		1.32 (Hb, m)	8, 9, 11, 12	9, 12
11	11.7 CH_3	0.49 (t, 7.3)	9, 10	7, 9, 10a, 10b, 12	11.9 CH_3	0.85 (t, 7.3)	9, 10	9, 10a, 10b
12	17.4 CH_3	1.06 (d, 6.9)	8, 9, 10	9, 10a, 10b	17.2 CH_3	0.78 (d, 6.9)	8, 9, 10	9, 10a, 10b
13	23.7 CH_3	1.65 (s)	1, 7a, 8	7, 9[f]	23.4 CH_3	1.62 (s)	1, 7a, 8	7
14	176.7 C				176.7 C			
4-OH		17.28 (s)	3[f], 3a, 4, 5, 14			17.32 (s)	3a, 4, 5, 14	
6-OH		14.73 (s)	5, 6, 7, 7a[f]			14.88 (s)	5, 6, 7	

[a] Assignments are based on extensive 2D NMR measurements (HMBC, HSQC, COSY) in $(CD_3)_2CO$ and CD_3OD. [b] $(CD_3)_2CO$, 75.5 MHz. [c] $(CD_3)_2CO$, 500 MHz. [d] Numbers refer to carbon resonances. [e] Data obtained from selective NOESY and selective ROESY experiments. [f] Weak correlation.

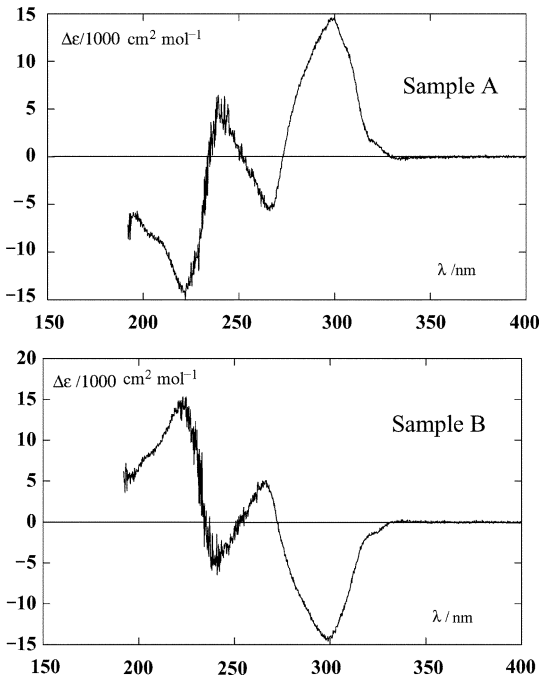

Fig. 1 Measured CD spectra: sample A, ascolactone A (**1**); sample B, ascolactone B (**2**).

C-9 of **1** and **2** a TDDFT-based method was applied.[16] In a first attempt, the flexible *sec*-butyl side chain was replaced with a hydrogen atom (see model compound **7** in Chart 1) and the configuration at C-1 was regarded as *R*. The two most stable conformers of 12 possibilities found through a conformational search have a relative energy of 1.58 kcal mol^{-1} at the MP2/6-311++G**//HF/6-31+G* level, resulting in Boltzmann factors of 0.909 and 0.063 at 298 K. For these two isomers, the electronic transition energies and the rotational strengths were then calculated with the TDDFT method employing the B3LYP functional and the TZVP basis set.[16] The averaged calculated CD curve of these isomers is shown in Fig. 2. The calculated spectrum has a positive Cotton effect at 291 nm followed by a negative one at about 241 nm. These effects are comparable in position and intensity to the experimental CD spectrum of **1** (Fig. 1) with a positive Cotton effect at 300 nm followed by a negative one at 265 nm, and we conclude that the configuration of carbon atom C-1 of ascolactone A (**1**) is very likely *R*.

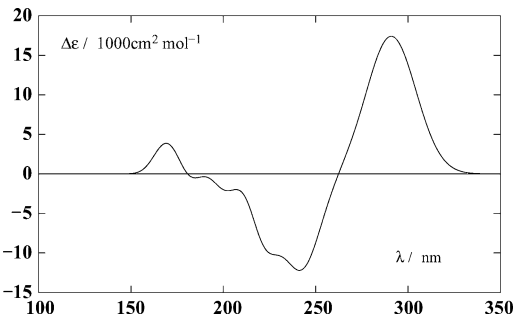

Fig. 2 Calculated (B3LYP/TZVP//HF/6-31+G*) CD spectrum of the 1*R* model compound (**7**). The two most stable conformers out of 12 were used to generate the spectrum. The Boltzmann factors have been calculated at the MP2/6-311++G**//HF/6-31+G* level.

To study the influence of the *sec*-butyl side chain, the aldehyde hydrogen of the most stable conformer was replaced by the either *S*- or *R*-configured (C-9) *sec*-butyl side chain of ascolactone A (**1**). Starting from these structures we performed conformational searches including only the dihedral angles θ_5 = C9–C8–C1–C7a, θ_6 = C12–C9–C8–C1 and θ_7 = C10–C9–C8–C1 and obtained 18 stationary points for (1*R*,9*R*) and 24 for (1*R*,9*S*). Using these structures as starting points in subsequent geometry optimizations at the HF/6-31+G* level resulted in 11 local minima for (1*R*,9*R*) and 12 for (1*R*,9*S*). We then calculated the CD spectra of all those structures of both series which are energetically not more than 3 kcal mol^{-1} (MP2/6-311++G**//HF/6-31+G*) above the corresponding most stable one [six for (1*R*,9*R*) and eight for (1*R*,9*S*)]. The corresponding CD curves obtained as Boltzmann-weighted superpositions are shown in Fig. 3. Both CD curves are strikingly similar, and it is almost impossible to distinguish them visually in the range above 200 nm.

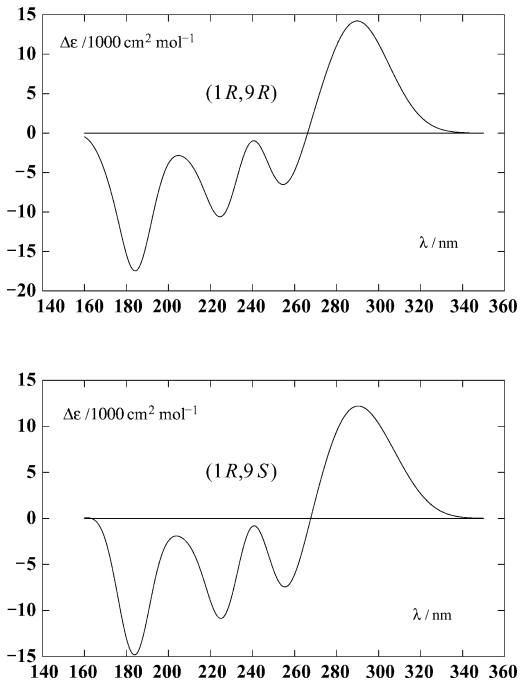

Fig. 3 Averaged CD spectra of (1*R*,9*R*) and (1*R*,9*S*) ascolactone calculated with the TDDFT using the B3LYP functional, the TZVP basis set and HF/6-31+G* geometries. The Boltzmann-weighted CD spectra of the six and eight most stable conformers have been superimposed to obtain the averaged spectra of (1*R*,9*R*) and (1*R*,9*S*), respectively. The corresponding Boltzmann factors have been calculated at the MP2/6-311++G**//HF/6-31+G* level.

While our calculations for the 1*R* isomer reproduce the signs and also approximately the λ_{max} of the first two Cotton effects measured for **1**, we were unable to reproduce the short wavelength region of the spectrum. This might be a result of the high flexibility of the side chain or/and of the solvent effects which were not taken into account in these calculations. The latter have been omitted since we do not believe that one of the commonly used electrostatic solvent models will be sufficient for a molecule like ascolactone where specific interactions with a solvent such as methanol might be important. However, since the calculations do approximate the long-wavelength region of the CD spectrum measured for

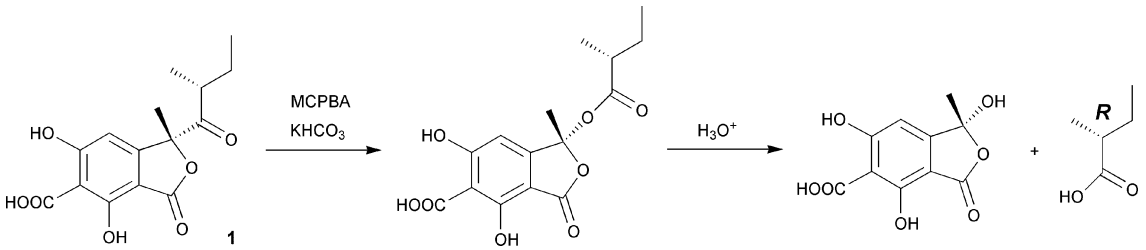

Scheme 1 Reaction scheme of Baeyer–Villiger oxidation and hydrolysis of ascolactone A (**1**).

ascolactone A (**1**), we conclude that **1** has either the (1*R*,9*R*)- or (1*R*,9*S*)-configuration.

The absolute configuration at C-9 of ascolactone A (**1**) was independently determined by Baeyer–Villiger oxidation of the side chain carbonyl and subsequent hydrolysis of the resulting ester (Scheme 1). Chiral GC–MS identified *R*-(−)-2-methylbutyric acid as the reaction product. Thus, the configuration at C-9 was assigned as *R*. Consequently, ascolactone A (**1**) and its epimer ascolactone B (**2**) are (1*R*,9*R*)- and (1*S*,9*R*)-configured, respectively.

In most cases, biosynthetic processes yield enantiomerically pure compounds. The occurrence of diastereomeric natural products produced during the same fermentation, as observed in the current study, is rare and probably the result of chemical equilibria during biosynthesis. Feeding experiments with [1,2-$^{13}C_2$]acetate in a liquid biomalt medium yielded ^{13}C-enriched ascochital (**5**) and ascosalipyrone (**6**) (Scheme 2, ^{13}C abundance approx. 8%). The labelling pattern of compounds **5** and **6** was deduced from the homonuclear couplings in the ^{13}C NMR spectra (Table 2), and showed the compounds to be derived from a single hexaketide and pentaketide chain, respectively. For compound **6**, a labelling experiment with [Me–^{13}C] methionine (^{13}C abundance approx. 80%) allowed the deduction that all methyl groups (except for CH_3-11) were derived from SAM (*S*-adenosyl-methionine) (Scheme 2, Table 2). Unfortunately, in the extracts obtained from the labelling experiment which have to be produced by liquid cultivation, compounds **1** and **2** could not be detected, probably because their formation requires solid media. The biosynthesis of **1** and **2** is, however, inferred from that of **5** and **6**. The presence of diastereomeric compounds, *i.e.* compounds **1**, **2**, **5** and **6** can be explained as a result of keto–enol tautomerism during biosynthesis (Scheme 2).

In silico screening is a promising approach to identify the putative biological activity of compounds. Using the PASS software,[9] polyketides **1**–**6** were identified as potential phosphatase inhibitors. The probability of inhibiting phosphatases was especially high for compounds **4** and **5** (Pa value >80%). Thus, **1**–**6** were tested towards a range of eukaryotic and prokaryotic protein phosphatases, *i.e.* Cdc25A (cell division cycle 25A) protein phosphatase, PTP1B (protein tyrosine phosphatase 1B), MPtpA and MPtpB (mycobacterial protein tyrosine phosphatases A and B),[3,4,17] VE-PTP (vascular endothelial protein tyrosine phosphatase)[18] and VHR (human *Vaccinia virus* VH1-related) dual-specific protein phosphatase. Ascochitine (**4**) inhibited MPtpB with an IC_{50} of 11.5 μM, and PTP1B with an IC_{50} of 38.5 μM. Other compounds were weak phosphatase inhibitors or were inactive (Table 3).

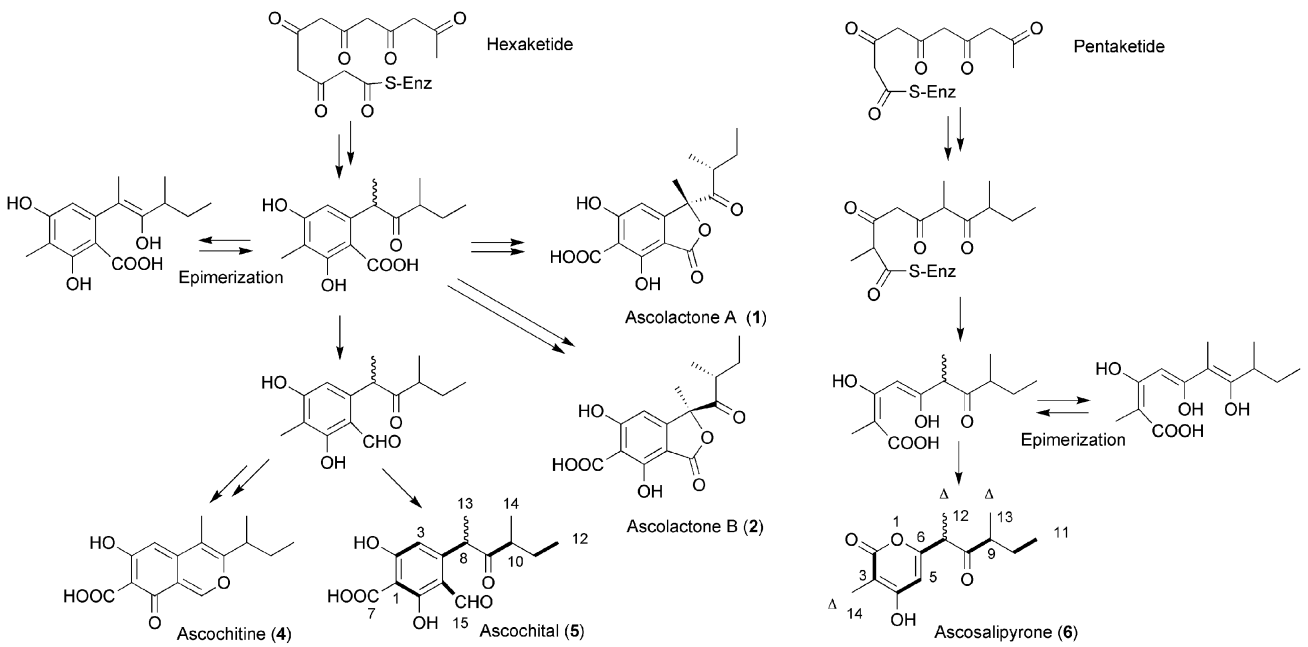

Scheme 2 ^{13}C labelling pattern of compounds **5** and **6** and proposed biosynthetic scheme for *A. salicorniae* metabolites (bold lines: carbons derived from intact acetate unit, Δ: methyl groups derived *via* SAM).

Table 2 ^{13}C NMR data for isotopically-labelled **5** and **6** [δ in ppm, J in Hz, $(CD_3)_2CO$, 75.5 MHz]

	5				**6**			
No.	$\delta\ ^{13}C$ [a]	$^1J_{C,C}$ [a,b]	$\delta\ ^{13}C$ [c]	$^1J_{C,C}$ [b,c]	$\delta\ ^{13}C$ [a]	$\delta\ ^{13}C$ [c]	$^1J_{C,C}$ [a,b,c]	$^1J_{C,C}$ [a,c,d]
1	102.9	63.1	102.9	63.1				
2	168.9	65.9	168.9	65.9	165.2	165.2	77.4	
3	107.9	65.9	107.8	65.9	99.4	99.4	77.4	47.2
4	148.5	38.4	148.7	38.4	164.6	164.7	57.6	
5	113.1	57.1	113.1	57.1	101.1	101.1	57.6	
6	171.0	63.1	171.0	63.1	161.5	161.7	51.0	
7	177.1		177.1		49.9	50.3	51.0	34.6
8	45.4	38.4	47.0	38.4	210.8	210.9	40.6	
9	213.2	39.0	213.7	39.5	46.9	46.8	40.6	33.5
10	46.8	39.0	46.3	39.5	26.3	26.8	35.1	
11	25.9	35.1	27.5	34.6	11.8	11.8	35.1	
12	11.9	35.1	11.7	34.6	14.4	14.3		34.6
13	17.5		16.2		16.8	16.2		33.5
14	17.6		17.4		8.5	8.6		47.2
15	190.3	57.1	190.2	57.1				

[a] Data of diastereomer A. [b] [1,2-$^{13}C_2$]acetate-enriched. [c] Data of diastereomer B. [d] [Me-^{13}C]methionine-enriched.

Table 3 Phosphatase inhibitory activities of compounds **2**–**5** [a]

Compound	Cdc25a [b]	PTP1B [b]	MPtpB [b]
2	n.a. [c]	n.a.	95.0 ± 10.0 [d]
3	n.a.	n.a.	87.8 ± 6.4 [e]
4	69 ± 9 [d]	38.5 ± 6.5 [e]	11.5 ± 1.3 [d]
5	n.a.	n.a.	61.2 ± 11.1 [e]

[a] Compounds **2**–**5** were also tested against the phosphatases VHR, MPtpA and VE-PTP and were found to be inactive. Compounds **1** and **6** were inactive towards all seven phosphatases. [b] $IC_{50}/\mu M$, $\pm$ standard deviation. [c] n.a.: not active. [d] $n = 3$. [e] $n = 4$.

Experimental

General experimental procedures

HPLC was carried out using a Merck-Hitachi system consisting of an L-6200 A pump, an L-4500 A photodiode array detector and a D-6000 A interface, together with a Knauer K-2300 differential refractometer as the detector or a system composed of a Waters 515 pump and a Knauer differential refractometer. ^1H (1D, 2D COSY, selective NOESY, selective ROESY, 2D NOESY) and ^{13}C (1D, DEPT 135, 2D HSQC, 2D HMBC) NMR spectra were recorded on Bruker Avance 300 DPX and Bruker Avance 500 DRX spectrometers in $(CD_3)_2CO$ and CD_3OD. Spectra were referenced to residual solvent signals with resonances at $\delta_{H/C}$ 2.04/29.8 [$(CD_3)_2CO$] and $\delta_{H/C}$ 3.35/49.0 (CD_3OD). UV and IR spectra were obtained employing Perkin-Elmer Lambda 40 and Perkin-Elmer Spectrum BX instruments, respectively. Optical rotations were measured with a Jasco DIP 140 polarimeter. CD spectra were taken on an AVIV 62DS. HREI-MS were recorded using a Kratos MS 50 spectrometer. LC–ESI-MS analyses were accomplished on an Agilent 1100 system (column: Macherey-Nagel Nucleodur-100 C-18, 5 µm, 125 × 2 mm) with an API 2000 Triple Quadrupole LC/MS/MS (Applied Biosystems/MDS Sciex) and a DAD. HPLC columns were from Knauer (250 × 8 mm, Eurospher-100 Si, 5 µm and 250 × 8 mm, Eurospher-100 C_{18}, 5 µm) and Phenomenex [250 × 4.6 mm, Luna C_{18} (2), 5 µm]. Polygoprep 60–50 C_{18} from Macherey-Nagel and Merck silica gel 60 0.040–0.063 mm were used for vacuum liquid chromatography (VLC). Sephadex LH-20 material for column chromatography was obtained from Amersham Pharmacia Biotech AB. Chiral GC–MS analyses were accomplished on a Perkin-Elmer AutoSystem XL gas chromatograph linked to a Perkin Elmer Turbomass mass spectrometer using a Perkin Elmer Cyclosil B column (30 m, ID 0.25 mm, film 0.25 µm).

Isolation and taxonomy of the fungus

Isolation and taxonomy of the fungus have been described previously.[8]

Cultivation

The fungus was cultivated in Fernbach flasks on a solid medium containing 20 g L^{-1} biomalt extract, 15 g L^{-1} agar and 80% artificial seawater at room temperature for 52 d. The artificial seawater contained (g L^{-1}): KBr (0.1), NaCl (23.48), $MgCl_2 \cdot 6H_2O$ (10.61), $CaCl_2 \cdot 2H_2O$ (1.47), KCl (0.66), $SrCl_2 \cdot 6H_2O$ (0.04), Na_2SO_4 (3.92), $NaHCO_3$ (0.19) and H_3BO_3 (0.03).

Extraction and isolation

Cultivation medium (8 L) and mycelia were extracted with ethyl acetate (3 × 8 L) after being homogenized using an Ultra Turrax T45. The ethyl acetate extract (3.2 g, brown oil) was fractionated by vacuum liquid chromatography (VLC) on RP-18 material with a gradient from MeOH–H_2O (10 : 90) to MeOH in 10 steps and then DCM to yield 11 fractions. Fractions 3 and 4 were combined because of their similar ^1H NMR spectra. The combined fractions (600 mg) were further separated with isocratic HPLC on silica gel [column: Knauer Si Eurospher-100, 250 × 8 mm, 5 µm, petroleum ether–acetone (40 : 60), 2 mL min^{-1}] to yield four fractions. Further purification of HPLC-fraction 2 by reversed-phase HPLC [column: Knauer C_{18} Eurospher-100, 250 × 8 mm, 5 µm, MeOH–H_2O (30 : 70), 2.5 mL min^{-1}], yielded the pure compounds **1** (11.3 mg), **2** (4.2 mg) and **5** (86.0 mg).

VLC fraction 6 was further separated by isocratic column chromatography on Sephadex LH-20 material (60 × 2.5 cm, MeOH) to yield 19 fractions. Fractions 5 and 6 of the separation on Sephadex were combined and purified by HPLC [column: Phenomenex Luna C_{18} (2), 250 × 4.6 mm, 5 µm, MeOH–H_2O (55 : 45), 1 mL min^{-1}] to yield 12.2 mg of pure hyalopyrone (**3**).

The pure metabolites **4** and **6** were isolated from a second ethyl acetate extract (2.8 g) obtained from 8 L of medium. The extract was fractionated by gradient normal phase VLC [gradient 1: DCM–EtOAc (100 : 0, 90 : 10, 60 : 20, 50 : 50, 20 : 60, 0 : 100); gradient 2: EtOAc–MeOH (75 : 25) to MeOH in four steps] to yield 10 fractions. Further HPLC separation of fraction 3 [column: Knauer Si Eurospher-100, 250 × 8 mm, 5 µm, petroleum ether–acetone–EtOAc (85 : 10 : 5), 2 mL min^{-1}] yielded 24.0 mg of **6**. VLC-fraction 1 was further purified by a second normal phase VLC [gradient 1: petroleum ether–EtOAc (100 : 0, 90 : 10, 60 : 40, 30 : 70, 20 : 80); gradient 2: EtOAc–acetone (100 : 0, 90 : 10, 70 : 30, 30 : 70, 0 : 100)] and yielded 89.1 mg of ascochitine (**4**).

CD spectra of ascolactone A (1) and B (2)

CD spectra were recorded in methanol at room temperature. The concentrations of both samples were 2.5×10^{-3} mol L^{-1} and the path length was 0.05 cm. A background correction was performed by substracting the spectrum of the neat solvent recorded under identical conditions.

Baeyer–Villiger reaction of ascolactone A (1)

Ascolactone A (**1**) (4.6 mg) was dissolved in 200 µL DCM–MeOH (50 : 50), treated with 3.5 mg MCPBA and 2.0 mg $KHCO_3$, and shaken at 120 rpm. Since no reaction product could be detected after 24 h, the temperature was steadily increased from 38 to 60 °C over the reaction period of 9 d. Also, an additional 3.5 mg MCPBA and 2.0 mg $KHCO_3$ were added after 24 and 144 h, respectively. An aliquot of the reaction mixture was analyzed by chiral GC–MS (column: Perkin Elmer Cyclosil B, 30 m, ID 0.25 mm, film 0.25 µm; 70 °C for 2.5 min, gradient 70–155 °C in 42.5 min) and compared with standards of S-(+)-2-methylbutyric acid (retention time 20.9 min) and racemic 2-methylbutyric acid (retention times 20.9 and 21.3 min). Chiral GC–MS identified *R*-(−)-2-methylbutyric acid as the reaction product.

Incorporation of [1,2-$^{13}C_2$]acetate into ascochital (5) and ascosalipyrone (6)

The fungus was grown in 1000 mL shake flasks, each of which contained 200 mL of liquid biomalt medium (20 g L^{-1} biomalt extract in 80% artificial seawater). The flasks were shaken at 25 °C and 90 rpm. 0.02 g [1,2-$^{13}C_2$]acetate in aqueous solution was added five times to every flask every 12 h starting from the 84 hour-old culture. After 10 d, the culture was extracted five times with the same volume of ethyl acetate. The ethyl acetate extract (1.0 g, brown oil) was fractionated by VLC on RP-18 material with a gradient of MeOH–H_2O (10 : 90) to MeOH in 10 steps and then DCM to yield 11 fractions. Purification of fraction 4 by HPLC [column: Knauer Si Eurospher-100, 250 × 8 mm, 5 µm, petroleum ether–acetone (60 : 40), 2 mL min^{-1}] yielded 42.9 mg of labelled ascochital (**5**). Separation of VLC fraction 5 by HPLC [column: Knauer Si Eurospher-100, 250 × 8 mm, 5 µm, petroleum ether–acetone–EtOAc (85 : 10 : 5), 2 mL min^{-1}] gave 4.7 mg of labelled ascosalipyrone (**6**). The abundance of ^{13}C in the labelled metabolites was approximately 8%.

Incorporation of [Me-^{13}C]methionine into ascosalipyrone (6)

The fungus was cultured as described for the incorporation of [1,2-$^{13}C_2$]acetate. 0.02 g [Me-^{13}C]methionine in aqueous solution was added five times to every flask every 12 h starting from the 96 hour-old culture. After 9 d the culture was extracted as described above and yielded 0.6 g of ethyl acetate extract. The crude extract was separated into 10 fractions by VLC as described above except for the gradient starting with MeOH–H_2O (20 : 80). Fraction 5 was further purified by HPLC [column: Knauer Si Eurospher-100, 250 × 8 mm, 5 µm, petroleum ether–acetone (65 : 35), 2 mL min^{-1}] to yield 10.5 mg of labelled ascosalipyrone (**6**) (^{13}C abundance approx. 80%).

Ascolactone A [(1*R*,9*R*)-4,6-dihydroxy-1-methyl-1-(2-methylbutanoyl)-3-oxo-1,3-dihydro-2-benzofuran-5-carboxylic acid] (1)

White amorphous solid (11.3 mg, 0.35%); $[\alpha]_D^{25}$ +156.4 (*c* 0.7 in MeOH), $[\alpha]_D^{22}$ +172.7 (*c* 0.7 in EtOAc); CD λ_{max} (MeOH)/nm: 220 (1000 cm^2 mol^{-1}, −15), 240 (+5), 265 (−5), 300 (+15); UV λ_{max} (MeOH)/nm: 232 (ε/dm^3 mol^{-1} cm^{-1}, 21 176), 260sh (8478), 311 (4073); IR (ATR) ν_{max}/cm^{-1}: 3443 (OH), 1716 (CO), 1718 (CO); ^1H and ^{13}C NMR data (see Table 1); LRESI-MS *m*/*z*: 309 $(M + H)^+$; LREI-MS *m*/*z*: 264 (60), 179 (100); HREI-MS *m*/*z*: 264.1000 $(M^+ - CO_2)$ (calc. for $C_{14}H_{16}O_5$: 264.0998).

Ascolactone B [(1*S*,9*R*)-4,6-dihydroxy-1-methyl-1-(2-methylbutanoyl)-3-oxo-1,3-dihydro-2-benzofuran-5-carboxylic acid] (2)

White amorphous solid (4.2 mg, 0.13%); $[\alpha]_D^{25}$ −169.2 (*c* 0.5 in MeOH), $[\alpha]_D^{22}$ −174.6 (*c* 0.5 in EtOAc); CD λ_{max} (MeOH)/nm: 220 (1000 cm^2 mol^{-1}, +15), 240 (−5), 265 (+5), 300 (−15); UV λ_{max} (MeOH)/nm: 232 (ε/dm^3 mol^{-1} cm^{-1}, 21 042), 260sh (8324), 311 (3997); IR (ATR), ν_{max}/cm^{-1}: 3452 (OH), 1720 (CO), 1722 (CO); ^1H and ^{13}C NMR data (see Table 1); LRESI-MS *m*/*z*: 309 $(M + H)^+$; LREI-MS *m*/*z*: 264 (15), 179 (100); HREI-MS *m*/*z*: 264.0998 $(M^+ - CO_2)$ (calc. for $C_{14}H_{16}O_5$: 264.0998).

Hyalopyrone (3)

Yellowish solid (12.2 mg, 0.38%); $[\alpha]_D^{27}$ −16.6 (*c* 1.0 in MeOH), [lit.[19] −15.9 (*c* 0.22 in MeOH)], ^1H, ^{13}C NMR, UV and IR data (see ref. 10), ESI-MS *m*/*z*: 225 $(M + H)^+$.

Ascochitine (4)

Yellow solid (89.1 mg, 3.18%); $[\alpha]_D^{27}$ −65.4 (*c* 0.1 in $CHCl_3$) [lit.,[12] −86 (*c* 1.0 in $CHCl_3$)]; ^{13}C NMR, UV and IR data (see refs. 13 and 20), ESI-MS *m*/*z*: 277 $(M + H)^+$.

Ascochital (5)

Brown-yellow solid (86.0 mg, 2.69%); ^1H, ^{13}C NMR, UV and IR data (see ref. 14), ESI-MS *m*/*z*: 295 $(M + H)^+$.

Ascosalipyrone (6)

White solid (24 mg, 0.86%); ^{1}H, ^{13}C NMR, UV and IR data (see ref. 8); ESI-MS m/z: 239 $(M + H)^+$.

Activity prediction

In silico screening was carried out *via* the WWW interface of the PASS (prediction of activity spectra for substances) software.[9]

Enzyme assays

Expression and purification of protein phosphatases VHR, PTP1B and Cdc25A. Expression plasmid VHR-1-pT7 for human VHR phosphatase was a gift from J. Denu (University of Wisconsin, Madison, USA). For protein production, plasmid was transformed into *E.coli* strain BL21-CodonPlus(DE3)-RIL (Stratagene) and grown on LB medium containing 100 μg mL^{-1} ampicillin and 35 μg mL^{-1} chloramphenicol. The protein expression was induced at an optical density of 0.6 at 600 nm, by addition of IPTG to 0.4 mM, and the bacteria are grown for an additional 6 h at 37 °C. Cells were lysed in buffer A [100 mM 2-(4-morpholino)ethanesulfonic acid, pH 6.5, 1 mM EDTA, 1 mM DTT] by passing twice through a fluidizer (Microfluidics) and the lysate was cleared by centrifugation. The supernatant was loaded onto a 50 mL S-Sepharose cation-exchange column pre-equilibrated with buffer A and the enzyme was eluted with linear NaCl gradient. Fractions containing phosphatase were concentrated and loaded onto a Superdex G-75 gel filtration column equilibrated with 50 mM HEPES, 40 mM NaCl, 1 mM EDTA (pH 7.4) and 1 mM DTT. Eluted fractions containing a single band of VHR were concentrated and stored in multiple aliquots at −80 °C.

Expression plasmid pT7-PTP1B for human PTP1B phosphatase was a gift from Z. Zhang (Indiana University, Indianapolis, USA). Transformation into *E.coli*, protein expression and purification was performed as described for CDC25A.

Expression plasmid pET9A-CDC25A for human Cdc25A phosphatase was a gift from I. Hoffmann (German Cancer Research Center, Heidelberg, Germany). Protein expression and lysate preparation was performed as described above except IPTG was added to 0.1 mM and expression was performed for 16 h at 20 °C. Cells were lysed in lysis buffer [50 mM Na_2HPO_4, pH 8.0, 0.3 M NaCl and 2 mM β-mercaptoethanol (BME), 1 mM PMSF] and loaded onto a 5 mL Hi-Trap Ni Sepharose column (Pharmacia) pre-equilibrated with the lysis buffer. Protein was eluted with a linear 5 to 200 mM imidazol gradient in 30 column volumes. Fractions containing Cdc25A were pooled and dilysed against 25 mM Tris pH 8.0, 100 mM NaCl, 1 mM BME and 5% glycerol, concentrated and stored in multiple aliquots at −80 °C.

All enzyme assays were performed by means of an automated system consisting of a Zymark SciClone ALH 500 in conjunction with a Twister II and a Bio-Tek Power Wave 340 reader. The reaction volume was 10 μL. The reaction was started by the addition of 5 μL *p*-nitrophenyl phosphate to 5 μL of a solution containing the respective enzymes which had been pre-incubated for 10–15 min with different concentrations from two-fold dilution series of inhibitors.

Reaction velocity was determined from the slope of the absorbance change at 405 nm and was related to control values in the absence of the inhibitor. IC_{50} values were obtained as 50% of the control from linear extrapolations of the initial reaction velocity as a function of the logarithmic of the concentration. This non-biased approach did not allow for the determination of IC_{50} values larger than 100 μM. The error indicated in Table 3 is the standard deviation of independent experiments. The overall experimental error, including the water content of the DMSO stock solutions and weighing errors, is approximately 50% of the respective IC_{50} values.

All buffered enzyme solutions contained 2 mM DTE (1,4-dithio-D,L-threitol added on the day of the experiment from 100 mM stock) and 0.025% (v/v) of the detergent NP-40 (Calbiochem 492015). The buffers consisted of 50 mM Tris, 50 mM NaCl, 0.1 mM EDTA in the case of Cdc25A and VE-PTP, or 25 mM HEPES, 50 mM NaCl, 2.5 mM EDTA in the case of PTP1B, MPtpA and MPtpB, or 25 mM MOPS, 5 mM EDTA in the case of VHR. The two-fold dilution series were obtained from 10 μL of a buffered enzyme solution containing 200 μM of inhibitor. Of this, 5 μL were removed and mixed with 5 μL buffered enzyme solution resulting in a two-fold dilution. This step was repeated five times. A 5 μL aliquot of the final dilution was removed, so that each well consisted of 5 μL of the buffered enzyme inhibitor mix. After addition of 5 μL *p*-nitrophenyl phosphate, the concentrations for the enzyme reaction were 50 mM in the case of Cdc25A or 1 mM for all other phosphatases. The inhibitor concentrations were 100, 50, 25, 12.5, 6.25 or 3.125 μM, respectively. For all enzymes, their concentration was adjusted with respect to their activity to an initial velocity of 1–2 OD_{405} h^{-1}. All reactions were performed as quadruplicates from identical manual dilutions (1 : 10 in buffer from 10 mM stock solutions in DMSO).

Acknowledgements

We thank Professor Dr D. Vestweber, Max-Planck-Institute for Molecular Biomedicine, Münster for providing the VE-PTP and Professor Dr H. Schwalbe and Dr K. Saxena, Institute for Organic Chemistry and Chemical Biology, University of Frankfurt for providing MPtpA and MPtpB. We are also grateful to Dr G. Eckhardt and C. Sondag, Institute for Chemistry, University of Bonn for making all EI-MS measurements. This project is part of the Graduiertenkolleg GRK677 'Struktur und molekulare Interaktion als Basis der Arzneimittelwirkung' and is financially supported by the Deutsche Forschungsgemeinschaft (DFG).

References

1 L. Bialy and H. Waldmann, *Angew. Chem., Int. Ed.*, 2005, **117**, 3880–3906.
2 T. O. Johnson, J. Ermolieff and M. R. Jirousek, *Nat. Rev. Drug Discovery*, 2002, **1**, 696–709.
3 R. Singh, V. Rao, H. Shakila, R. Gupta, A. Khera, N. Dhar, A. Singh, A. Koul, Y. Singh, M. Naseema, P. R. Narayanan, C. N. Paramasivan, V. D. Ramanathan and A. K. Tyagi, *Mol. Microbiol.*, 2003, **50**, 751–762.
4 M. Manger, M. Scheck, H. Prinz, J. P. von Kries, T. Langer, K. Saxena, H. Schwalbe, A. Fürstner, J. Rademann and H. Waldmann, *ChemBioChem*, 2005, **6**, 1749–1753.
5 R. E. Cebula, J. L. Blanchard, M. D. Boisclair, K. Pal and N. J. Bockovich, *Bioorg. Med. Chem. Lett.*, 1997, **7**, 2015–2020.
6 A. Loukaci, I. Le Saout, M. Samadi, S. Leclerc, E. Damiens, L. Meijer, C. Debitus and M. Guyot, *Bioorg. Med. Chem.*, 2001, **9**, 3049–3054.
7 K. A. Alvi, A. Casey and B. G. Nair, *J. Antibiot.*, 1998, **51**, 515–517.

8 C. Osterhage, R. Kaminsky, G. M. König and A. D. Wright, *J. Org. Chem.*, 2000, **65**, 6412–6417.
9 D. A. Filimonov, V. V. Poroikov, Y. V. Borodina and T. A. Gloriozova, *J. Chem. Inf. Comput. Sci.*, 1999, **39**, 666–670; V. V. Poroikov, D. A. Filimonov, Y. V. Borodina, A. A. Lagunin and A. Kos, *J. Chem. Inf. Comput. Sci.*, 2000, **40**, 1349–1355; V. V. Poroikov, D. Akimov, E. Shabelnikova and D. A. Filimonov, *SAR QSAR Environ. Res.*, 2001, **12**, 327–344; http://www.ibmc.msk.ru/PASS/.
10 P. Venkatasubbaiah and W. S. Chilton, *J. Nat. Prod.*, 1992, **55**, 461–467.
11 S. Bertini, *Ann. Sper. Agrar.*, 1956, **11**, 545–556.
12 H. Oku and T. Nakanishi, *Phytopathology*, 1963, **53**, 1321–1325.
13 L. Colombo, C. Gennari, G. Severini Ricca, C. Scolastico and F. Aragozzini, *J. Chem. Soc., Perkin Trans. 1*, 1980, 675–676.
14 C. Kusnick, R. Jansen, K. Liberra and U. Lindequist, *Pharmazie*, 2002, **57**, 510–512.
15 G. Raabe, C. Repges, Y. Wang and J. Fleischhauer, *Enantiomer*, 2002, **7**, 77–83; Y. Wang, J. Fleischhauer, S. Bausch, M. Sebestian and P. H. Laur, *Enantiomer*, 2002, **7**, 347–374; E. N. Voloshina, Y. Wang, N. A. Voloshin, G. Raabe, H.-J. Gais and J. Fleischhauer, *Z. Naturforsch., A: Phys. Sci.*, 2003, **58**, 443–450; Y. Wang, G. Raabe, C. Repges and J. Fleischhauer, *Int. J. Quantum. Chem.*, 2003, **93**, 265–270; E. N. Voloshina, G. Raabe, J. Fleischhauer, G. J. Kramp and H.-J. Gais, *Z. Naturforsch., A: Phys. Sci.*, 2004, **59**, 124–132; M. G. Bröckelmann, J. Dasenbrock, B. Steffan, W. Steglich, Y. Wang, G. Raabe and J. Fleischhauer, *Eur. J. Org. Chem.*, 2004, 4856–4863; M. Albrecht, I. Janser, J. Fleischhauer, Y. Wang, G. Raabe and R. Fröhlich, *Mendeleev Commun.*, 2004, 250–252; E. Voloshina, G. Raabe, M. Estermeier, B. Steffan and J. Fleischhauer, *Int. J. Quantum. Chem.*, 2004, **100**, 1104–1113; E. Voloshina, J. Fleischhauer and P. Kraft, *Helv. Chim. Acta*, 2005, **88**, 194–209; D. Enders, M. Milovanovic, E. Voloshina, G. Raabe and J. Fleischhauer, *Eur. J. Org. Chem.*, 2005, 1984–1990.
16 S. F. Seibert, G. M. König, E. Voloshina, G. Raabe and J. Fleischhauer, *Chirality*, 2006, DOI: 10.1002/chir.20266.
17 D. Müller, A. Krick, S. Kehraus, M. Hart, F. C. Küpper, H. Prinz, P. Janning, H. Waldmann, H. Schwalbe, K. Saxena and G. M. König, *J. Med. Chem.*, submitted.
18 R. Nawroth, G. Poell, A. Ranft, S. Kloep, U. Samulowitz, G. Fachinger, M. Golding, D. T. Shima, U. Deutsch and D. Vestweber, *EMBO J.*, 2002, **21**, 4885–4895.
19 Y. Wang and J. B. Gloer, *J. Nat. Prod.*, 1995, **58**, 93–99.
20 I. Iwai and H. Mishima, *Chem. Ind.*, 1965, 186–187.

